CRASHWORTHINESS OF TRUNCATED COMPOSITE CONES UNDER SIDE LOADS

David C. Fleming* **and Anthony J. Vizzini†**

Center for Rotorcraft Education and Research
Composites Research Laboratory
Department of Aerospace Engineering
University of Maryland
College Park, MD 20742, USA

ABSTRACT

Truncated cones of varying degrees of taper were manufactured from unidirectional AS4/3501–6 graphite/epoxy preimpregnated tape and were loaded in compression. Different amounts of side loads were introduced by orienting the loading axis away from the central axis of the cone. The cones were crushed under quasi-static conditions, and their energy absorption was measured. For small amounts of taper, the energy absorbency decreases with increasing amounts of side load. There is also an increasing tendency toward toppling. As the amount of taper is increased, the energy absorbency properties are better maintained through the range of side loads applied. Furthermore, the tendency for toppling is reduced. Thus, optimization of a crashworthy structure with constant cross section specimens characterized solely by uniaxial tests can result in poor performance during a crash event. However, optimization using tapered cross sections results in a structure capable of absorbing energy during a uniaxial crushing event as well as an event with substantial amounts of side loads.

INTRODUCTION

Crashworthiness is one of the foremost goals of rotorcraft design. In order to provide a high level of protection to the occupants in the event of a crash, a system oriented design approach is often used whereby the aircraft system in its entirety is designed for the crash event. This generally includes the landing gear, the seat substructure and the fuselage assembly. These components absorb crash energy through a wide variety of mechanisms ranging from the deflection and deformation of structural elements to the failure of these elements. The energy absorption of a rotorcraft structure in a crash is a highly complex process dependent upon the specific failure processes which the energy absorbing components undergo [1]. These mechanisms must in general depend not only on the materials used in the construction of the components and the specifics of their design, but also the attitude and velocity of the vehicle at impact. Crashworthiness requirements were developed to account for the variety of crash conditions. MIL-STD-1290, for example, specifies that occupants be protected in vertical impact of up to 12.8 meters per second at aircraft attitudes within ±10° roll and +15°/–5° pitch [2]. The crashworthiness of the aircraft as a whole is dependent on the response of the various components which absorb the energy of the crash. The loads experienced by these components are highly complex in any crash situation and vary significantly through the structure. These loads in general are not axial and include a component perpendicular to the axes of the structure. This has a considerable effect on the failure mechanisms of the structure, consequently altering its energy absorbing capability. In order to design components for crashworthy structures it is necessary to understand the effects of these side loads on the structure, as well as the other complexities introduced by non-axial loadings.

Composite materials have a potential application in the sub-floor structures of rotorcraft [1,3-4]. Under axial crushing loads, composite materials can have energy absorbing capabilities by weight superior to aluminum [5,6]. Thus the possibility exists of using composite materials to provide the desired crashworthiness characteristics of a structure while preserving or even enhancing the performance of the vehicle. The effects of side loads, however, must be considered. In the presence of side loads a

* Minta Martin Fellow
† Assistant Professor

non-uniform stress distribution exists even around a symmetric component. This stress distribution can induce local buckling in the component. In this case, crushing failure initiates at certain locations on the cross section rather than around the whole perimeter. The crushing process itself is also affected by the presence of side loads, and the moment induced by the side loads produces a tendency for global failure. Previous research has demonstrated that components loaded in the presence of side loads experience changes in failure mechanisms. This affects the energy absorption capacity of the structure by reducing both the total amount of energy absorbed by the structure and the rate at which the energy is absorbed [7].

Since any misalignment is dependent on the many complexities involved during a crash event, the precise loading condition would vary significantly even in similar events. Thus, analytical prediction of the loading condition is pointless. If a structure is optimized solely for axial loads, then during an off-design crash event the performance of the structure would be severly degraded. This lost performance can be recaptured by altering the geometry of the components. Structures optimized with consideration of side loads and the resulting moments may have reduced energy absorbency under axial loads but will provide improved performance through a broader range of crash conditions.

Since the reduction in energy absorption of the structure is due to a misalignment between the load path and the material which undergoes crushing, a realignment of all or part of the material to the applied load would increase the performance.

The truncated cone is a configuration which partially realigns the energy absorbing material to the unknown loading condition. In this way, part of the structure still undergoes the type of crushing which has been well characterized in uniaxial specimens. It is the purpose of this study to examine the energy absorption capability of tapered geometries through a range of off-axis loading conditions.

TEST SPECIMENS

Truncated cone specimens were tested to investigate the effect of taper on the energy absorption of composite structures over a range of loading conditions. A typical specimen is shown schematically in Figure 1. Two angles describe the specimen: the taper angle, ψ, and the load inclination angle, ϕ. A crushing load, P, applied normal to the ends results in a normal compressive force of $P\cos\phi$ and a side load of $P\sin\phi$ in the axis system of the component. A toppling moment about the end of the central axis is also created by this loading and is equal to $PL\sin\phi$, where L is the height of the specimen measured normal to the ends. Since the truncated cone is cut at an angle relative to its central axis, the resulting cross section is elliptical. Moreover, the angle which the cone makes with the loading plane varies around the circumference reaching a minimum and a maximum value at the ends of the major axis of the ellipse. Thus, a coordinate system is defined. The angle α is measured positive counter clockwise when viewing the specimen from the top, *i.e.*, the smallest cross section. The coordinate is zero at the point where the length along the truncated cone is maximized as shown in Figure 1.

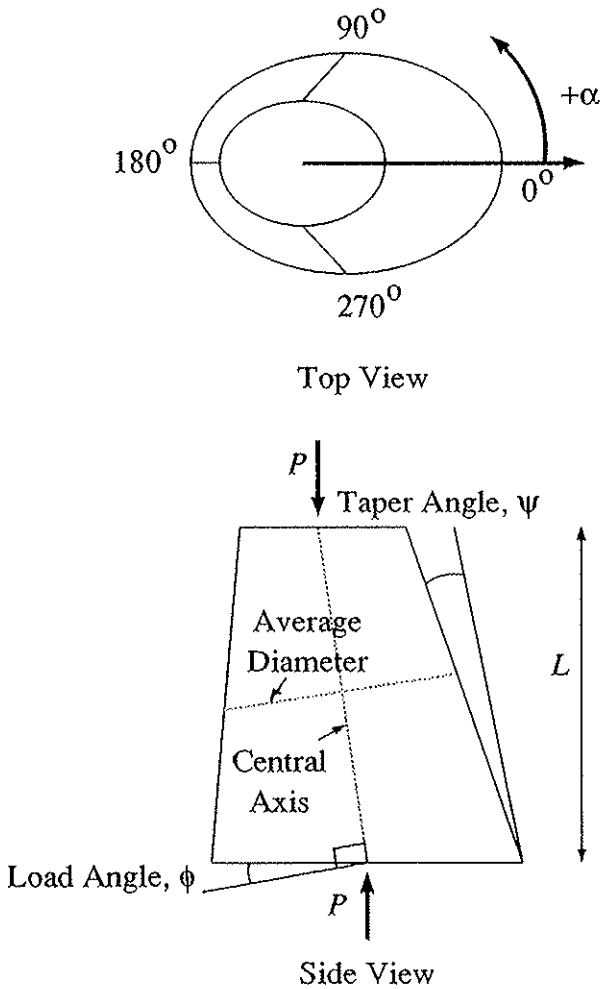

Figure 1 Schematic of the truncated cone specimen

Specimens were manufactured with taper angles, ψ, of 1°, 5° and 10°. The 1° taper angle was chosen to approximate the behavior of a cylindrical specimen. The taper in each case allows easy removal of parts from aluminum mandrils after cure. Each mandril had a 150 mm-long tapered section and approximately 75 mm of constant diameter stock at each end to allow for easy handling of the cure assembly during layup. The specimens used in this study had a length of 102 mm measured along the line where α equals zero and had an average diameter of 38.1 mm.

The specimens were manufactured at the Composites Research Laboratory at the University of Maryland. Net resin Hercules AS4/3501-6 graphite/epoxy preimpregnated tape was hand wrapped around aluminum mandrils to form $[\pm 45/0]_S$ specimens. This layup is similar to that used by other researchers [4,5,8] and is well behaved in compression. Failure is dominated by brooming at the ends and in-plane fracture as opposed to ply buckling, delamination, and shell buckling [8].

If strips of preimpregnated tape were to be wrapped around the mandril, a variation of the angle orientation would result because the specimens do not have a constant cross section. Narrow strips of tape could be wrapped around the mandrils to form the plies in the 1° taper cases. However, for 5° and 10° taper cones thin strips wrapped around the mandrils at nonzero fiber angles change orientation drastically in the axial direction. Moreover, the desired 45° plies in the 5° and 10° taper cones cannot be made with continuous fiber strips for the given dimensions of the specimens. If the ply were to be wrapped from the larger diameter end to achieve the desired 45° angle at some point along the cross section, the orientation would change so severely as to reverse the direction of the wrapping along the longitudinal axis. A wrap begun at any initial angle from the smaller diameter end rapidly approaches an axial orientation.

A nearly uniform layup in both the circumferential and axial directions was made by forming each ply from separate trapezoidal pieces of preimpregnated tape butted against each other. Figure 2 shows a schematic of a typical ply. A ply formed in this way wraps around the mandril covering it completely. The center line of each trapezoidal piece is used as a reference line when cutting the pieces. The angle of the ply is given with respect to this

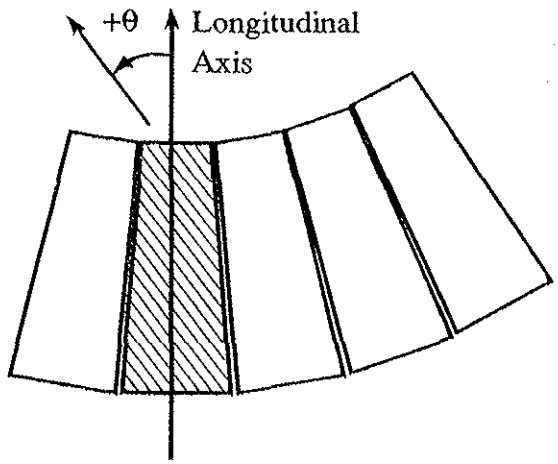

Figure 2 Trapezoidal pieces which form a ply of a hand-layup truncated cone

reference line. Within a single piece, the angle orientation on the surface of the mandril varies slightly in the circumferential direction. The amount of this variation is constant along an axial projection. Specimens laid up in this fashion, therefore, have a layup that varies slightly around the circumference and is constant along each axial line.

Six trapezoidal pieces per ply were chosen in order to keep the maximum angle variation in the circumferential direction in the most extreme case, the 45° plies in the 10° taper specimens, to approximately ±10% while minimizing the number of pieces in each ply. The pieces were sized such that the first completed ply, composed of six equally sized pieces, wrapped around the mandril exactly. In subsequent plies, to account for the increasing diameter of the part to be covered, the last piece in each ply was made larger to fill in the extra space. Since laying up plies in this fashion creates discontinuities running along the length of the specimen, each ply was laid on one half ply width in the circumferential direction away from the previous so that successive fiber breaks would not lie atop of each other.

Laid–up specimens were covered with peel ply then wrapped with non-porous Teflon film. All seams of the Teflon film were sealed with flash tape to prevent resin leakage. Specimens were then tightly wrapped in air breather, to minimize surface irregularities imposed by the cure materials, and sealed in a vacuum bag. Specimens were cured in an autoclave using the manufacturer's recommended cure cycle of one hour at 116 °C and two hours at 177 °C under 0.586 MPa autoclave pressure with

a full vacuum drawn in the bag. Specimens were then postcured in an oven for eight hours at 116 °C without pressure or vacuum.

To load the specimens under compressive loads with an adjustable amount of side load, the ends of the specimens were cut at an angle with respect to the central axis of the specimen. The specimens were cut with a Bridgeport milling machine equipped with an aluminum table and a diamond grit blade with water cooling. A diagram of the cutting arrangement is shown in Figure 3. With this arrangement, the ends are cut parallel to each other. Specimens were clamped to a piece of channel stock attached to the milling machine table perpendicular to the plane of the blade. The blade was then angled with respect to the central axis, taking care to account for the taper angle of the specimen. The bottom edge of a truncated cone resting on the straight channel is not parallel to the surface of the mill table for a non-zero taper angle. Measurements showed that this angle was slight for small degree of taper specimens. For the 10° taper specimens, a correction of +1° of blade rotation was necessary to obtain the proper cuts. Based on previously reported results, both ends to the specimen were chamfered with a belt sander to approximately 60° to reduce the peak load before crushing and to allow damage to initiate freely at either end [4].

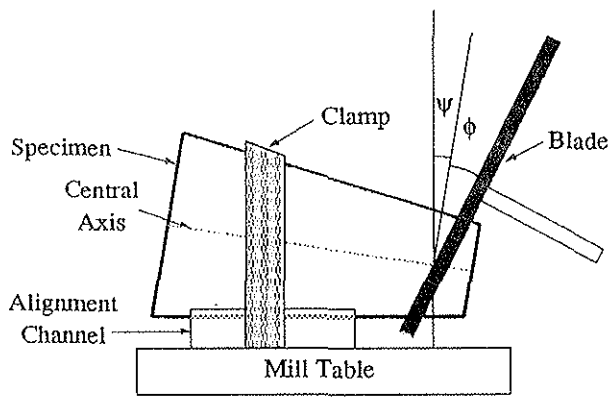

Figure 3 Diagram of the specimen cutting arrangement

A total of 20 specimens with discontinuous trapezoidal ply wraps were manufactured. Specimens were made with end cut angles, ϕ, of 0°, 5°, 10° and 20°. Two specimens of each cut angle were made for the 5° and 10° taper angle cases and one of each cut angle was made with a 1° taper angle. Each specimen was instrumented with four EA-06-125AD-120 strain gages oriented in the loading direction. Gages were located at α equal to 0°, 90°, 180° and 270°. In addition, previous results [7] of 1° taper specimens with continuous ply wraps are included to compare the effects of different manufacturing processes on energy absorption.

Each of the specimens was placed between self-aligning platens on an MTS 810, 220 kip testing machine. They were quasi-statically crushed at a constant stroke rate of 0.0635 mm/sec. The process was allowed to continue until the specimens either had been crushed to 50 percent of their original length or had toppled. The crushing load, the stroke and strain gage data were automatically recorded at 0.5 second intervals. From this data it is possible to evaluate the energy absorption characteristics of the specimens as a function of the taper angle and the load inclination angle.

RESPONSE

Specimens exhibited two types of behavior during the tests: crushing and toppling. Crushing behavior was evident to some degree in all of the specimens. Toppling behavior appeared only in cases where the load inclination angle exceeded the taper angle and is characterized by the rotation of the specimens about an axis perpendicular to the specimen central axis. This results in relatively little structural damage to the specimen. Differences between the phenomena are evident in the load-stroke, the strain-stroke, and the energy absorption response of the specimens.

Crushing

A typical plot of compressive load versus the compressive stroke for a specimen which exhibits only crushing behavior is shown in Figure 4. Load increases linearly until damage initiation. After the point of initiation, the load drops to a relatively low value while the stress is redistributed and the crushing process fully develops. Following this transition region, the load fluctuates about a linear path due to periodic damage and the continuation of the crushing process. These three regions characterize the load-stroke behavior of the specimens.

When a specimen has a non-zero taper angle, the amount of material being crushed varies with stroke. Typically, damage initiates at the smaller radius of the truncated cone. Thus as the crushing event progresses the amount of material to be

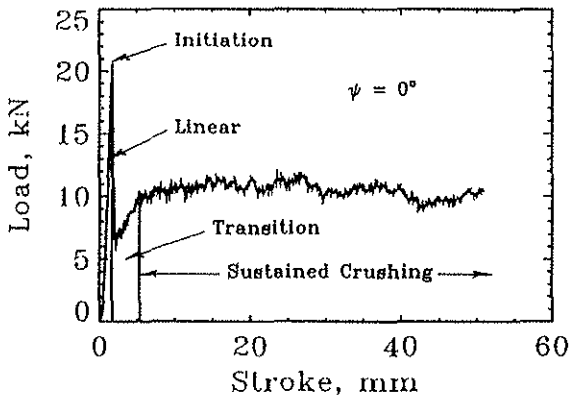

Figure 4 Typical load versus stroke plot indicating the distinct regions during crushing

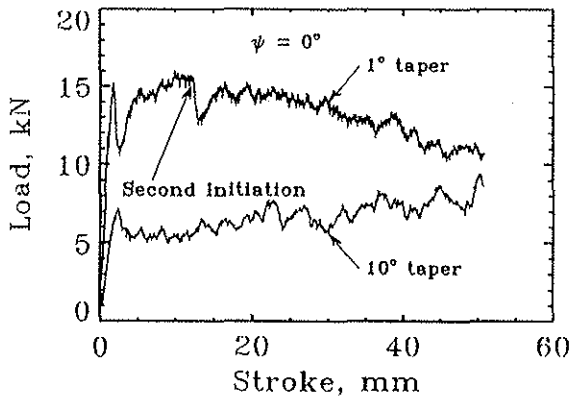

Figure 5 Typical load versus stroke indicating damage initiation at bottom and increasing crushing load

crushed increases. The change in crushed area is small for the 1° taper case and the load, therefore, remains fairly constant as shown in Figure 4. In the higher taper angle cases the effect of the change in specimen cross section becomes more pronounced producing a greater slope of the load-stroke curve as shown in Figure 5 for a 10° taper specimen. In a few cases, damage later initialized at the opposite end and is evident in the load stroke data by an abrupt drop in the crushing load. This drop is followed by a second transition region after which the load again stabilizes at a different slope as shown in Figure 5 for a 1° taper specimen.

Damage initiation was first visible as a number of short cracks running in the fiber direction along the edge of initiation. As the stroke increased after initiation, brooming developed along the edge of initiation. A lip of damaged material began to spread outward from the initiated sites. In the cases where crushing fully developed before toppling, the damage then spread around the entire cross section, forming a growing lip of damaged material bending away from the specimen. Powder size bits of material, as well as some larger pieces, dropped from the damaged area during the entire event. Examination of specimens after the tests showed that a variety of damage mechanisms contributed to the crushing process. There was evidence of delamination between plies, as well as fiber cracking. In general, little material from the crushed region remained intact, rather the material was broken into very small pieces. This is probably due in part to the discontinuities in the ply.

Differences exist in the initiation behavior between the axially loaded specimens (ϕ equal to 0°) and the specimens loaded with the addition of side loads within each taper angle case. In all taper angle cases the average initiation load generally decreased as the load inclination angle increased. The different taper angle cases, however, exhibited a difference in tolerance to damage initiation as the load angle increased. This behavior can be seen in Figure 6 which shows the initiation load versus load angle, ϕ, for each taper angle case. In general, a high initiation load reflects a broader region of damage at the onset of crushing. On the other hand, a low initiation load indicates the likelihood of toppling.

For the axially loaded specimens the smallest taper angle specimen had the greatest initiation load. By 10° load inclination angle, though, the 5° taper specimens initiated at a higher load than the 1° taper specimen. At 20° load inclination angle, both the 5°

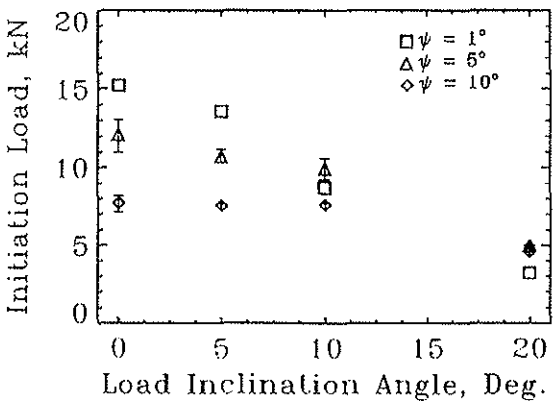

Figure 6 Initiation load versus load inclination angle

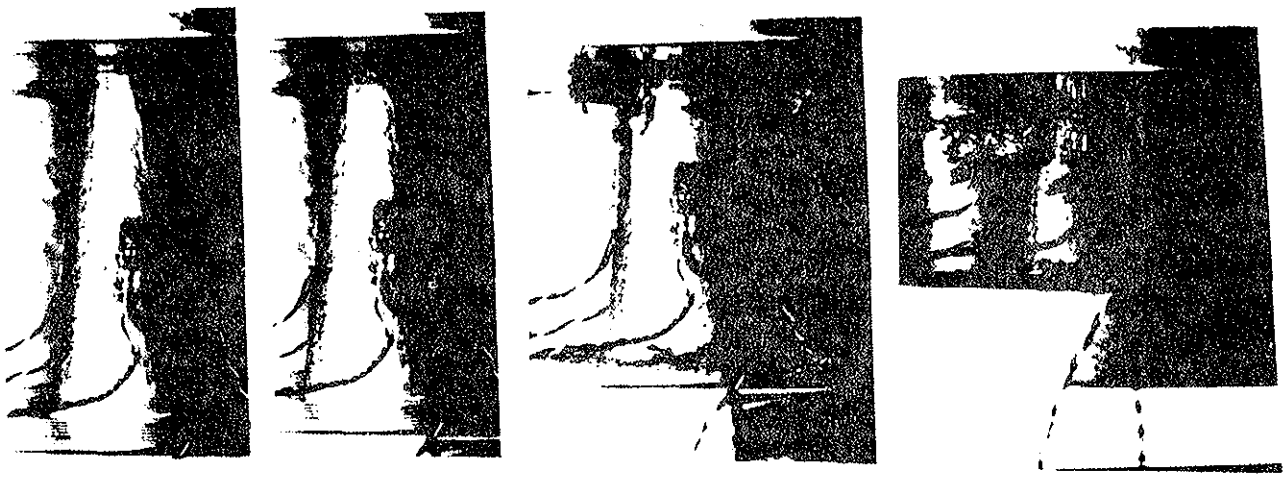

Figure 7 Photographs of the crushing sequence of a 5° taper specimen

and the 10° taper specimens had a greater initiation load than the corresponding 1° taper specimen. Also note that the load initiation value for the 5° load angle and the 10° load angle 1° taper specimens are each within 15% of the initiation load for the axially loaded 5° taper and the 10° taper specimens respectively, indicating a correlation between the angle which the side of the specimen makes with the contact surface and damage initiation.

Axially loaded specimens exhibited no preferred damage initiation site. Once initiated, brooming quickly encompassed the entire cross section. The damage then progressed from the end of damage initiation in a uniform fashion and post-mortem examination shows a nearly axially symmetric damage pattern. Figure 7 shows a sequence of photographs of a 5° taper specimen undergoing crushing at a load inclination angle of 0°.

In the off-axis loading cases, damage initiated at a preferred site: the top edge at α equal to 180°. Damage initiates at this preferred location as a result of a load concentration, and thus the damage initiation load is decreased. The first visible cracking appeared near the initiation site, and brooming was more readily apparent in this location immediately after initiation. In the off-axis specimens which sustained crushing, the cracks and brooming spread, encircling the entire cross section. The lip of damaged material was larger on the α equal to 180° side whereas in the α equal to 0° position the material tended to be pushed into the interior of the specimen.

Toppling

Toppling behavior appeared in specimens where the load inclination angle was greater than the taper angle. In all cases when the difference between the two angles was 10° or greater toppling occurred. The behavior is due to damage initiation on the bottom surface of specimens after initiation and crushing had begun on the top. In toppling, a local section of the bottom cross section sustains damage while the rest of the cross section remains intact. This damage sequence effectively removes material which serves to stabilize the structure. Thus, the structure is destabilized.

Toppling is characterized by the reduction of crushing damage and the increased tilting of the specimen. The top surface remains in contact while the undamaged portion of the bottom edge loses contact with the platen. The angle which the central axis of the specimen makes between the platens then increases until the change in geometry prevents the specimen from supporting any load. Then the specimen drops over. Figure 8 shows a sequence of photographs of a 5° taper specimen undergoing crushing and toppling at a load inclination angle of 10°.

Toppling can be seen in the load-stroke and strain-stroke curves. For example, in Figure 9 a 1° taper angle specimen at a 10° load inclination angle undergoes both sustained crushing and toppling. After displaying the typical crushing response, the load curve drops steeply as toppling begins to dominate the behavior of the specimen. The sharp spikes

Figure 8 Photographs of the toppling sequence of a 5° taper specimen

in the curve, characteristic of the periodic breaking of the fiber ends during crushing, disappear at this point. The structure can no longer effectively resist the applied load, and increasing the stroke tilts the specimen further.

The strain gage data in conjunction with the load-stroke curve show the point of toppling initiation. As the specimen begins to topple, pressure is relieved from the ends on the sides opposite the sites of maximum damage. As the toppling progresses, these sites, on the bottom surface at α equal to 0° and the top surface at α equal to 180°, lose contact with the crushing platens. Thus the strain drops to near zero on the α equal to 0° and 180° sides. The point at which the strain begins to drop monotonically to zero is the point of toppling initiation. This is shown in Figure 9 at the point when the stroke is approximately 23.4 mm. Note that after toppling initiates, the specimen still exhibits some crushing behavior. The strain gage at α equal to 90° indicates an increase at that location after toppling has started. Eventually, the strain at this location decreases to zero as the entire specimen topples. Strain gage data can thus be used to determine whether toppling behavior is present in a specimen and at what stroke it initiates. The crushing response of specimens can then be evaluated independently of toppling response by considering the regions before and after toppling initiation separately.

The overall crushing and toppling behavior of each type of specimen can be seen in the photographs in Figures 10 through 12. As discussed, crushing results in the destruction of the structure whereas toppling results in relatively little damage.

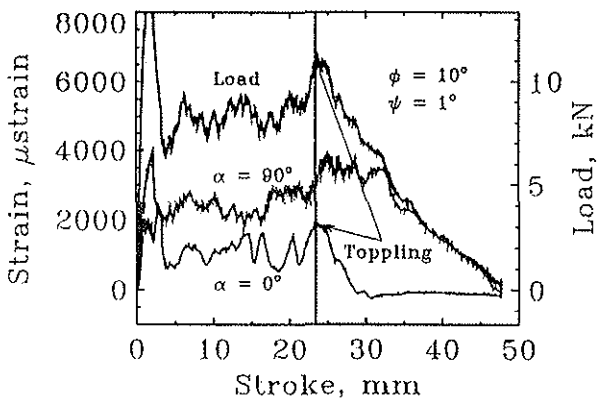

Figure 9 Load and strain versus stroke for a 1° taper specimen loaded at ϕ=10°

ENERGY ABSORPTION

The cumulative amount of energy absorbed by a specimen at a given point in the test is obtained by numerically integrating the load versus stoke response up to that point. A linear interpolation is assumed between successive data points. Energy versus stroke is presented in Figures 13 through 15 for each taper angle. The quadratic nature of the energy-stroke curves is evident within the sustained crushing regions. The effect is especially pronounced in the 10° taper case. The quadratic nature is due to the linear nature of the load versus stroke curves. The occurrence of toppling is indicated in these curves by the tangent slope approaching zero.

1° TAPER SPECIMENS

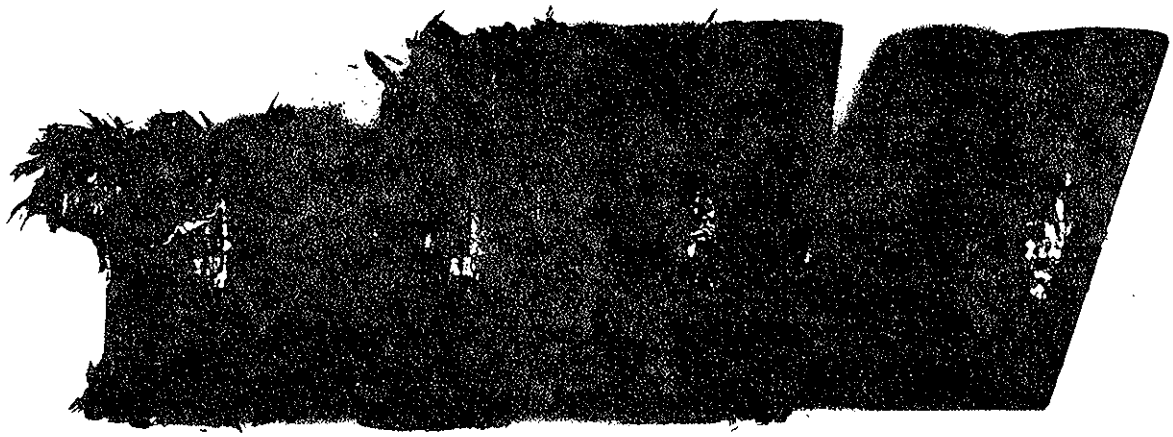

1-1 1-2 1-3 1-4

Figure 10 Photograph of the 1° taper specimens

5° TAPER SPECIMENS

5-1 5-2 5-3 5-4

Figure 11 Photograph of representative 5° taper specimens

The load and energy data can be standardized by the cross sectional properties of the specimens as a function of stroke in order to effectively compare the energy absorption properties of the different taper angle specimens. The specific crushing stress is obtained by dividing the load by the prod-

10° TAPER SPECIMENS

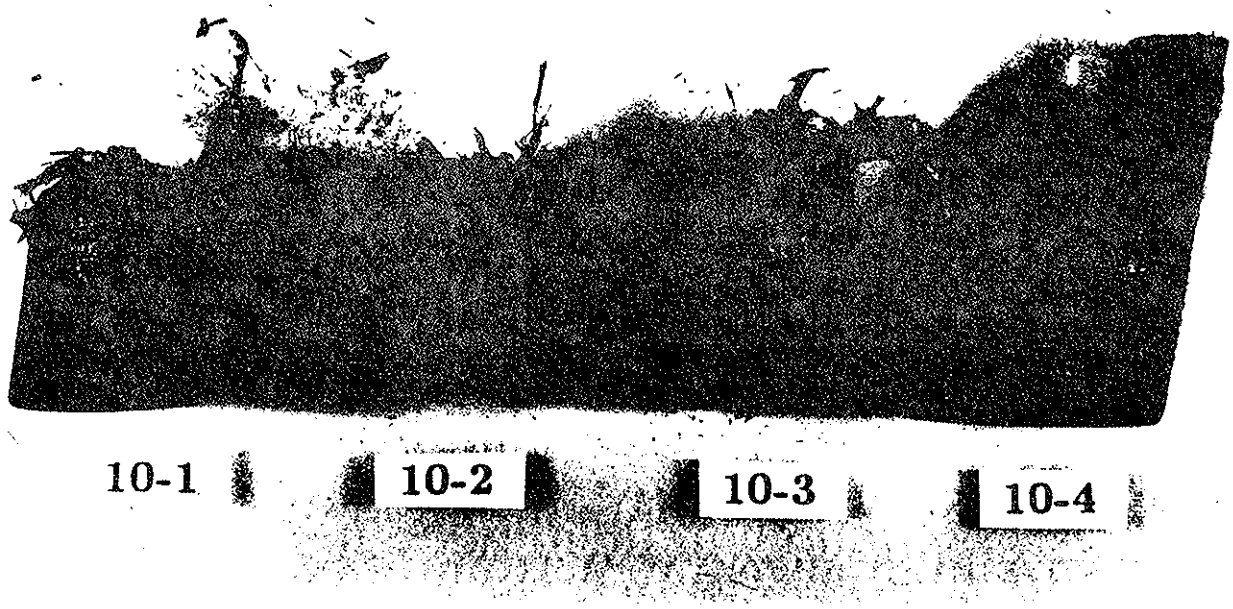

Figure 12 Photograph of representative 10° taper specimens

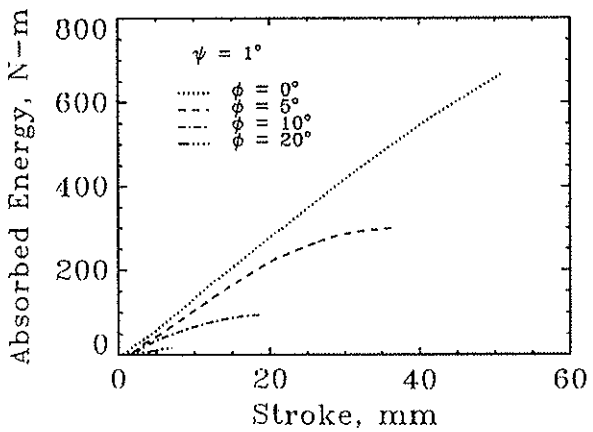

Figure 13 Energy versus stroke for 1° taper specimens

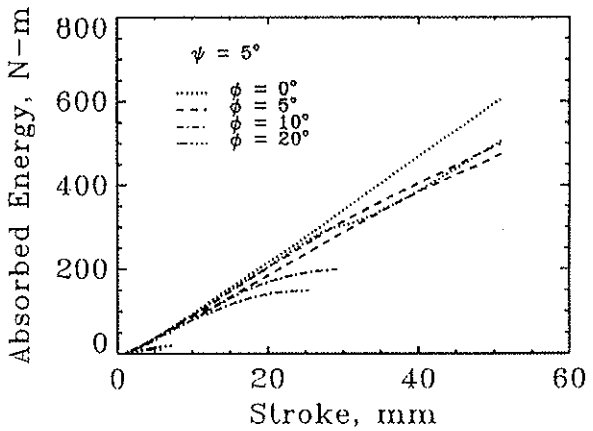

Figure 14 Energy versus stroke for 5° taper specimens

uct of the instantaneous cross section area of the region experiencing crushing and the density of the material. This value is equivalent to the instantaneous energy absorbed per unit mass of material destroyed. The average value of this specific crushing stress in the region of sustained crushing provides a measure of the energy absorption capacity of the structure and is presented in Figure 16. In the specimens in which failure initiated at the bottom after first crushing from the top, only the part of the sustained crushing region before the second initiation was considered when determining the specific crushing stress. No values of the specific crushing stress were obtained for specimens with a 20° load inclination angle because in each case specimens at that inclination toppled before developing a significant sustained crushing region.

The 1° taper specimens with plies composed of trapezoidal strips have a greater energy absorbing capacity than the 1° taper specimens with continuous-fiber plies. At each load inclination angle, the specimens with discontinuous plies have a greater specific crushing stress. Furthermore, for the continuous fiber layups, the specific crushing stress

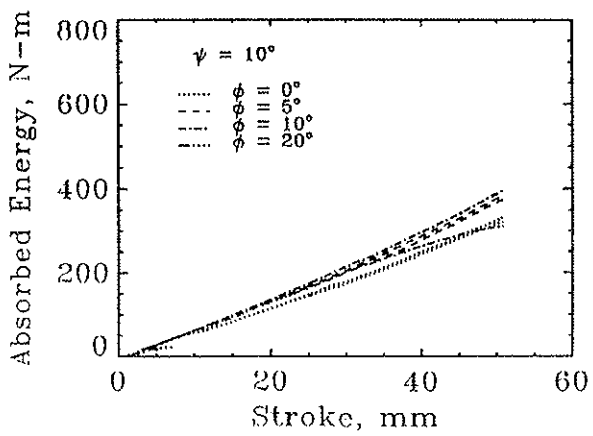

Figure 15 Energy versus stroke for 10° taper specimens

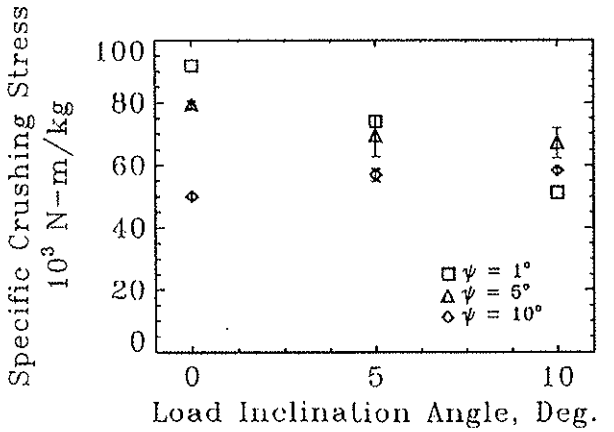

Figure 16 Specific crushing stress versus inclination angle for each taper angle

of the specimens at a load inclination angle of 0° was slightly less than the specific crushing stress at a load inclination angle of 5°. The reduced energy absorption capability is due to the tendency towards delamination in these specimens. In the specimens with discontinuous fibers, there is more of a tendency for the fibers to break.

Additionally, the value of the specific crushing stress obtained for the discontinuous fiber, 1° taper specimen is comparable to results obtained by other researchers for similar graphite/epoxy systems [5], although the specific layup and material choices are different. The superiority of the discontinuous ply layup over the continuous-wrapped specimens coupled with the similarity to previous results demonstrates that the discontinuous ply specimens provide good energy absorbing properties. It also suggests that the discontinuities in the plies may serve as an effective damage initiator, possibly enhancing the overall performance of the specimen.

The specific crushing stress data presented in Figure 16 follow similar trends to the initiation load data. In the axially loaded cases (ϕ equal to 0°) the performance is reduced as the taper angle increases. The 1° taper specimen has a 13% greater specific crushing stress than the 5° taper specimens. At a load angle of 5°, the 1° taper specimen still provides the greatest energy absorption capability, but the 5° taper specimen has only 5% lower specific crushing stress. By a 10° load inclination angle, however, the 5° taper specimen has surpassed the capability of the 1° taper specimen, providing 24% more capacity. In fact, at this inclination angle, even the 10° taper specimens have a greater specific crushing stress than the slightly tapered section. The greater load bearing capacity of the more highly tapered specimens at greater load inclination angles is due to the better alignment of parts of the structure with the load path. In such regions the structure is more likely to fail in a manner which absorbs more energy. Where the load is aligned with the structure there is more of a tendency toward fiber breakage than at steeply misaligned locations, where the fibers may more easily delaminate and bend away from the structure.

The energy versus stroke data can be standardized against the mass of material crushed through the given stroke. Energy absorbed per unit mass crushed is presented in Figures 17–19. Note that this data yields the approximate specific crushing stress and is presented to demonstrate that standardization yields a nearly constant energy absorbency rate throughout the sustained crushing region even in those cases which experienced a large stroke through the crushing region and regardless of the taper angle of the specimen. Thus the quadratic nature of the energy versus stroke curve is resolved. For specimens in which toppling initialized at the bottom after normal initialization, the behavior of the standardized energy curve is affected. This is because the standardization technique becomes invalid at this point.

Figure 20 shows the specific crushing stress plotted agains the initiation load for all of the specimens. Generally, specimens which initiate at a relatively high load tend to also exhibit higher specific crushing stress. Low values of the initiation load are indicative of a load concentration at a preferred location on the cross section. This concentration reduces in energy absorption because the damage to the structure is localized.

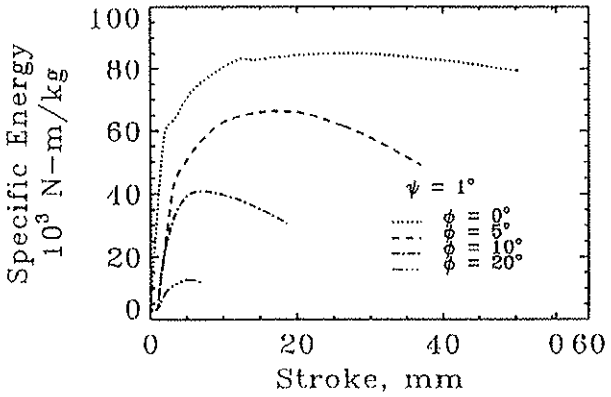

Figure 17 Specific energy absorption versus stroke for ψ=1°

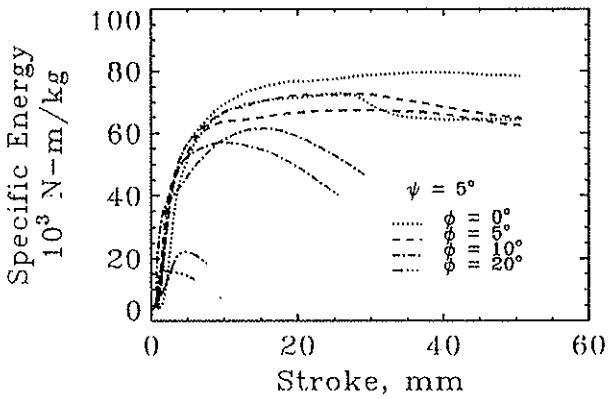

Figure 18 Specific energy absorption versus stroke for ψ=5°

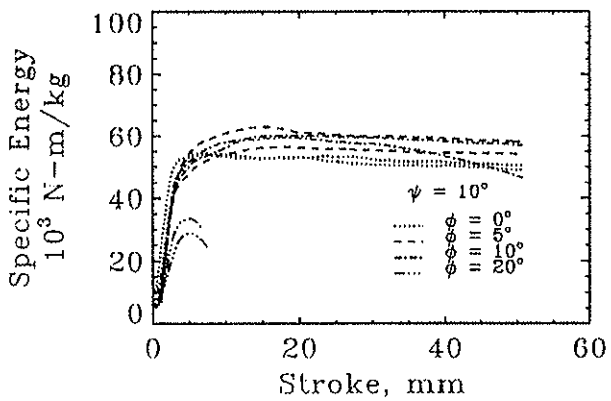

Figure 19 Specific energy absorption versus stroke for ψ=10°

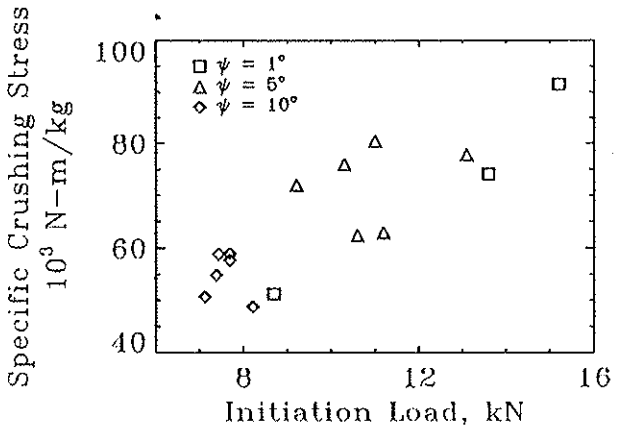

Figure 20 Specific crushing stress versus damage initiation load

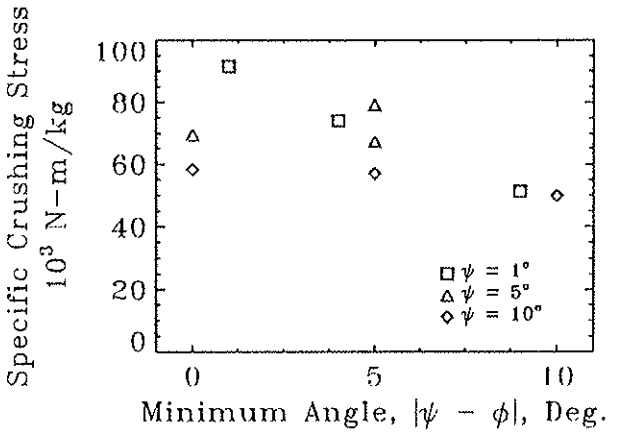

Figure 21 Specific crushing stress versus the minimum angle difference

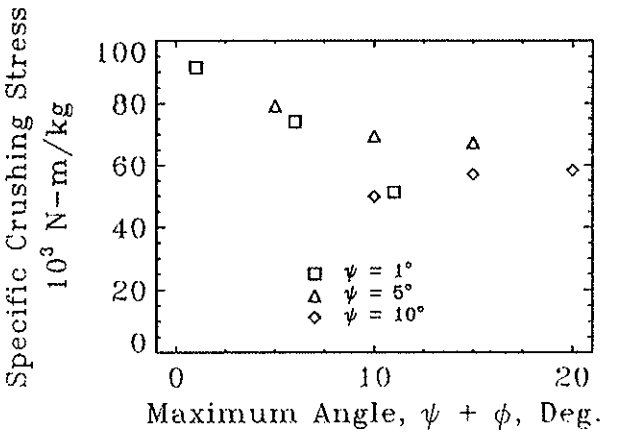

Figure 22 Specific crushing stress versus the maximum angle difference

Two possible parameters of interest are the minimum and maximum incident angle made by the load and any edge of the tapered specimen. The minimum is given by the absolute difference between the load inclination angle and the taper angle. The maximum value is given by the sum of the load inclination angle and the taper angle. These two newly defined angles indicate the degree of misalignment between the load and the cone. In Figures 21 and 22, the specific crushing energy is plotted

agains the absolute difference and the sum of the inclination angle and the taper angle. In general the trend is towards a decrease in performance as either of these two parameters increase. Thus as the load becomes more misaligned, the overall performance decreases.

As a global failure, toppling has a severe impact on the energy absorption properties of the specimens. Toppling both constrains the total useful stroke of the specimen and the its total energy absorption capacity. The specimens which toppled have significantly lower total energy absorption than the other specimens within their respective groups. Susceptibility to toppling was reduced with increasing taper angle. Toppling occurred for all of the off axis loadings in the 1° taper cases. In the 5° taper case, specimens at 10° and 20° load inclination angle cases toppled. Only the 20° load inclination case toppled of the 10° taper specimens. Thus, increasing taper angle effectively acts to resist toppling.

CONCLUSIONS

In a crashworthy design, the ability of the structure to absorb energy under complex loading conditions is vital to the efficient and safe design of the structure. The results presented herein indicate clearly that the presence of side loads is a limiting factor in the energy absorption properties of structures. However, the introduction of non-constant cross section elements can alleviate, in part, this limitation. In particular, the following conclusions can be made:

1. Several parameters have been identified which indicate the energy absorbing capability of the structure. In particular, an increase in the damage initiation load indicates an increase of the specific crushing stress and thus the specific energy capacity of the structure. Also an increase in either the minimum or maximum angles of incidence between the applied load and the edges of the specimen indicates a decrease in performance.

2. For slightly tapered, nearly cylindrical, specimens, as the load inclination angle increases the energy absorbing capacity decreases. These specimens also show an increasing tendency to topple as the load angle increases.

3. Increasing the taper angle, allows the structure to better maintain its energy absorption capabilities through a range of inclination angles. Additionally, the taper helps to reduce the tendency of the specimens toward toppling.

4. The increase in taper results in a reduction of the energy absorbing capacity of the structure under axial loads. However, due to their decreased sensitivity, the energy absorbing properties of the more highly tapered specimens approach and surpass those of the slightly tapered specimens as the load inclination angle is increased.

5. The linearly increasing nature of the load-stroke response of the tapered structure may also improve the overall crashworthiness of the structure. Tapered sections act as non-linear, strain-hardening springs. Since the crushing load increases during the event, the portion of the deacceleration imposed by the sub-floor assembly on the occupant is initially reduced at a time when the overall deacceleration is at a peak.

6. Given an anticipated level of side load, there is an optimal value for the taper of the structure. Moreover, designs which depend on constant cross sections characterized under uniaxial loadings may be fatally in error when the crash event includes off-designed side loads.

ACKNOWLEDGEMENTS

This work was supported in part through the Center for Rotorcraft Education and Research at the University of Maryland sponsored by the U.S. Army Research Office. The authors wish to thank Mr. William R. Pogue, III for his help in this effort.

REFERENCES

1. J.K. Sen, "Designing for a Crashworthy All-Composite Helicopter Fuselage," *Journal of the American Helicopter Society*, Vol. 32, No. 2, April 1987, pp. 56–66.

2. J.D. Cronkhite, "Design of Airframe Structures for Crash Impact," *Proceedings of the AHS National Specialist's Meeting on Crashworthy Design of Rotorcraft*, Atlanta, GA, April 7-9, 1986.

3. P.H. Thornton, "Energy Absorption in Composite Structures," *Journal of Composite Materials*, Vol. 13, July 1979, pp. 247-262.

4. G.L. Farley, "Energy Absorption of Composite Materials," *Journal of Composite Materials*, Vol. 17, May 1983, pp. 267-279.

5. G.L. Farley, "Energy Absorption of Composite Material and Structure," *Proceedings of the AHS 43rd Annual Forum*, St. Louis, MO, May 18–20, 1987, pp. 613–627.

6. J.K. Sen, C.C. Dremann, "Design Development Tests for Composite Crashworthy Helicopter Fuselage," *SAMPE Quarterly*, Vol. 17, No. 1, October 1985, pp. 29–39.

7. D.C. Fleming and A.J. Vizzini, "The Effect of Side Loads on the Energy Absorption of Composite Structures," *Proceedings 5th Technical Conference of the ASC*, East Lansing, MI, June 11–13, 1990, pp. 611–620.

8. A.J. Vizzini and P.A. Lagace, "The Role of Ply Buckling in the Compressive Failure of Graphite/Epoxy Tubes," *AIAA Journal*, Vol. 23, No. 11, November 1985, pp. 1791–1797.